

A Role of Filaments in the Axisymmetrization of an Isolated Two-Dimensional Elliptic Vortex with a Non-Uniform Vorticity Distribution

Shin-ya MURAKAMI and Takahiro IWAYAMA

Department of Earth and Planetary Sciences, Kobe University, Kobe, Hyogo

We numerically examine the role of filaments in the axisymmetrization of an isolated elliptic vortex with a non-uniform vorticity distribution for a two-dimensional incompressible barotropic fluid. To quantitatively examine the role of filaments in the axisymmetrization, we first divide the vorticity field into a core region and a surrounding region. The former corresponds to the core of the vortex, and the latter corresponds to the filaments and a weak vorticity region just outside the vortex core. Second, we analyze the radial displacement of the maximum and minimum curvature points on a vorticity contour in the core region advected by velocities induced by the vorticity of those regions. This investigation shows that the vorticity of the surrounding region largely contributes to the axisymmetrization at both points, especially when the filaments are forming. Thus, we conclude that the filaments play a significant role in the axisymmetrization of the isolated elliptic vortex.

1. INTRODUCTION

Large-scale atmospheric and oceanic motions on the earth are turbulent. Moreover planetary rotation and density stratification tend to make the atmospheric and oceanic motions horizontally two dimensional. To examine such aspects of atmospheric and oceanic motions, two-dimensional turbulence has been actively studied for a long time. It is well known that the vorticity field of decaying two-dimensional turbulence is full of long-lived and isolated vortices (McWilliams 1984¹). Thus, understanding vortex motion would be helpful for understanding two-dimensional turbulence.

Melander *et al.* (1987)² studied the axisymmetrization process of an isolated elliptic vortex with a non-uniform, positive vorticity distribution for a two-dimensional incompressible barotropic fluid. They regarded both a vorticity contour near the vortex core and the associated stream function contour near the vorticity contour as to be ellipses. Furthermore, they proposed the axisymmetrization principle,¹

$$\frac{dr}{dt}\phi_d \leq 0. \quad (1)$$

Here, r is the aspect ratio of the vorticity contour, and ϕ_d is the difference angle between the orientations of the vorticity contour and the nearby stream function contour. Because the velocity vector is tangent to the stream function contour, eq. (1) indicates that when $\phi_d > 0$, inward radial velocity is induced at the point of maximum curvature of the elliptic vorticity contour, whereas

¹If the elliptic vortex has negative vorticity, eq. (1) changes as $\frac{dr}{dt}\phi_d \geq 0$.

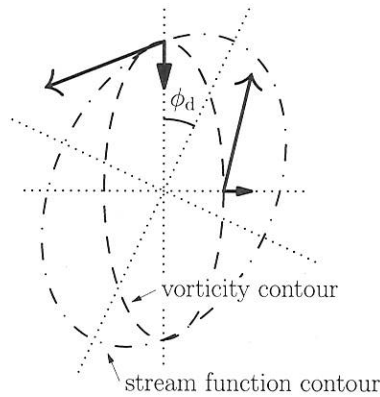


Figure 1: Schematic figure of a vorticity contour (ellipse with the broken line) and a nearby stream function contour (oblique ellipse with the dot-dashed line) for an elliptic vortex with positive vorticity. Solid lines indicate velocity vectors at the maximum and minimum curvature points on the vorticity contour and their projection to the radial direction of the vorticity ellipse.

outward radial velocity is induced at the point of minimum curvature (Fig.1). Therefore, when $\phi_d > 0$, the velocity field near the elliptic vorticity contour tends to axisymmetrize the vortex. The axisymmetrization principle was confirmed by their numerical experiments.²⁾

Melander *et al.* (1987)²⁾ discussed qualitatively that the angle ϕ_d can be non-zero when the vorticity field is distorted from the mirror symmetry of an ellipse due to the generation of filaments. Therefore, they concluded that isolated elliptic vortices relax toward axisymmetry as a result of filament generation. However, until now, no one has investigated the contribution of the filaments to ϕ_d and the quantitative relationship between ϕ_d and the velocity field on the vorticity contour.

In this study, we numerically investigate the axisymmetrization of an isolated elliptic vortex in a direct and quantitative fashion. We define a core region and a surrounding region, and we then investigate the contribution of those regions to the axisymmetrization of an elliptic vortex.

2. GOVERNING EQUATION AND SETTINGS OF THE NUMERICAL EXPERIMENT

In this section, we describe the governing equation and settings of our numerical experiment. Moreover, we describe a method for defining the core region and the surrounding region of the vortex.

2.1 GOVERNING EQUATION AND SIMULATION CONDITIONS

The governing equation is the vorticity equation for a two-dimensional incompressible barotropic fluid,

$$\frac{\partial \omega}{\partial t} + J(\psi, \omega) = \nu \nabla^2 \omega, \quad (2)$$

where ψ is the stream function, $\omega = \nabla^2 \psi$ is the vorticity, ν is the viscosity coefficient, and $J(\psi, \omega) = \partial_x \psi \partial_y \omega - \partial_y \psi \partial_x \omega$ is the Jacobian. The velocity field is given by $\mathbf{k} \times \nabla \psi$, where \mathbf{k} is the unit vector

perpendicular to the x - y plane. We apply doubly periodic boundary conditions to the rectangular domain with $2\pi \times 2\pi$. An initial vorticity field is given by

$$\omega(r) = \omega_0 \left[1 - \exp \left\{ -C \frac{R_0}{r} \exp \left(-\frac{R_0}{R_0 - r} \right) \right\} \right], \quad 0 \leq r < R_0, \quad (3)$$

where $r = \sqrt{ax^2 + by^2}$, and $\sqrt{a/b}$ is the initial aspect ratio of the vortex. We also set $C = -\frac{1}{2}e^2 \ln \frac{1}{2} \approx 2.5608517$, $R_0 = \pi/2$, $\omega_0 = 10$, $(a, b) = (10, 1)$, and $\nu = 1.5 \times 10^{-5}$. These parameter values are same as those for the compact-support case in Kimura and Herring (2001).³⁾

We use the third-order Adams-Bashforth scheme for time stepping and the pseudospectral method dealiased with the two-third rule at 3072^2 resolution. The vorticity equation (2) is integrated until $t = 15$.

2.2 DIAGNOSTICS

Until now, objective definitions of the core and filaments of a vortex were not known. Instead of a direct definition of the filaments, we divide the snapshot of the vorticity field into two parts, a core region and a surrounding region. We identify an outermost vorticity contour that remains elliptical throughout the integration and choose it as the boundary to divide the vorticity field into the core region and the surrounding region. Then, we define the core region such that $\omega(x, y) \geq \omega_{\text{th}}$ and the surrounding region as $\omega(x, y) < \omega_{\text{th}}$, where ω_{th} is the value of the vorticity of the outermost contour. For the appropriate threshold value that satisfied the above condition, we use $\omega_{\text{th}} = 6$. If we slightly vary the threshold value, the result presented below does not change qualitatively.

We consider the evolution of the vorticity contour with $\omega = 6, 7$ and 8 in the core region. We also focus on the stream function contours with values near the vorticity contours of interest. The values of the stream function contours are selected as the mean values of the stream function at the maximum and minimum curvature points of the vorticity contours.

The vorticity and the stream function contours of interest are regarded as ellipses similar to the work of Melander *et al.* (1987).²⁾ The contours are fit to ellipses by least-square fitting (Fitzgibbon *et al.* 1999⁴⁾).

In the two-dimensional turbulence, the Okubo-Weiss criterion (Okubo 1970⁵⁾; Weiss 1991⁶⁾) and the Hua-Klein criterion (Hua and Klein 1998⁷⁾) are often used to select the core regions of vortices.⁸⁾ When these criteria are solely used, they select not only a core region but also some fraction of the filaments. To remove some fraction of the filaments, additional conditions, for example the absolute value of the vorticity must be larger than a threshold value, or the pressure must be negative, are usually required.^{8, 9)} Instead, we use simpler method described above to extract the core region.

3. RESULTS AND DISCUSSION

3.1 A BRIEF OVERVIEW OF THE EVOLUTION OF THE ISOLATED VORTEX

In this section, we briefly describe the temporal evolution of the elliptic vortex. Fig.2 shows the time evolution of the vorticity field. Filaments are formed during the early stage of evolution, rotated around the vortex center with a slower speed than the vortex core, and simultaneously elongated. Filaments are formed again in $7 \lesssim t \lesssim 8$. At the end of the evolution, a weak vorticity region uniformly surrounds the vortex core. The aspect ratio of the vortex greatly decreases compared with the initial aspect ratio.

Fig.3 shows the time evolution of the aspect ratio of the vorticity contours, $\omega = 6, 7, 8$. The aspect ratio of the vorticity contours rapidly decreases until $t \lesssim 1.5$. After that, it oscillates during evolution with periods of $T = 1 \sim 1.8$.

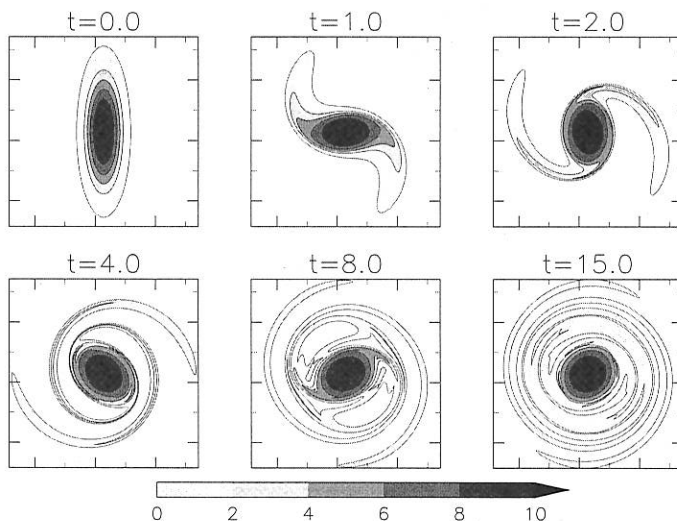


Figure 2: Time evolution of the vorticity field at some instant of time. Only a quarter of the computational domain is shown.

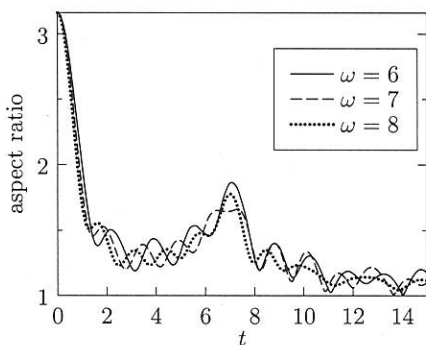


Figure 3: Time evolution of the aspect ratio of the vorticity contours with $\omega = 6$ (solid line), 7 (broken line), 8 (dotted line).

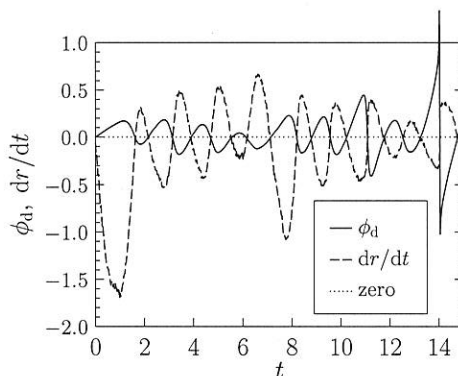


Figure 4: Time series of the difference angle, ϕ_d (solid line), and the rate of change of the aspect ratio, dr/dt (broken line), for the vorticity contour with $\omega = 6$.

Fig.4 shows the evolution of the difference angle, ϕ_d , and the rate of change of the aspect ratio, $\frac{dr}{dt}$. The axisymmetrization principle, $\phi_d \frac{dr}{dt} \leq 0$, proposed by Melander *et al.* (1987)²⁾ is well satisfied by our simulation.

Note that the aspect ratios of the vorticity contours show a short time increase in $6 \lesssim t \lesssim 7$. This can be explained by the reattachment of the filaments to the core, which generates a strong anti-mirror symmetric vorticity field near the core corresponding to $\phi_d < 0$.

Fig.5 and Fig.6 show the snapshots of the core region and the surrounding region of the vorticity field, respectively. Fig.5 shows that all of the vorticity contours in the core regions remain nearly

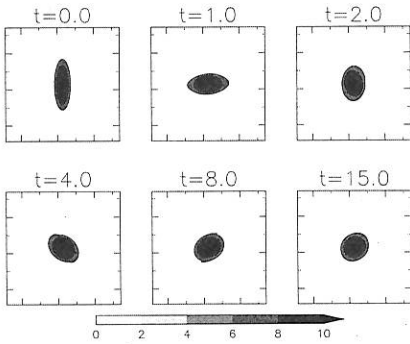


Figure 5: Snapshots of the vorticity field in the core region at the same time as Fig.2.

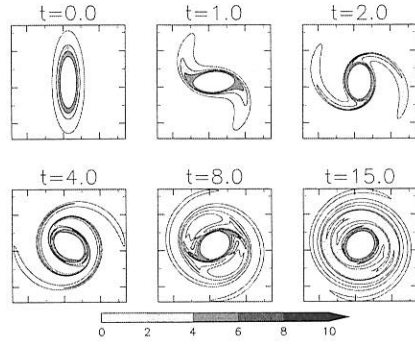


Figure 6: Snapshots of the vorticity field in the surrounding region at the same time as Fig.2.

elliptical; therefore, the core regions are successfully defined by the procedure described in section 2.2. Fig.6 shows that the surrounding regions consist of the filaments and the weak vorticity region around the core.

3.2 CONTRIBUTION OF FILAMENTS TO THE AXISYMMETRIZATION OF AN ELLIPTIC VORTEX

To reveal the axisymmetrization of an elliptic vortex, we focus on the deformations of vorticity contours in the core region by the vorticity of the core region and the surrounding region. First, we analyze the radial velocity at the maximum and minimum curvature points of the vorticity contours. We divide the velocity into two parts: the velocities induced by the vorticity field in the core region, $\mathbf{u}_c := \mathbf{k} \times \nabla \Delta^{-1} \omega_c$, and by those in the surrounding region, $\mathbf{u}_s := \mathbf{k} \times \nabla \Delta^{-1} \omega_s$, where ω_c and ω_s are the vorticity fields in the core region and the surrounding region, respectively. Using these velocities, we calculate the integral of the velocities with respect to time,

$$A_c(t) := \int_0^t \mathbf{u}_c(t') \cdot \mathbf{e}_r dt', \quad A_s(t) := \int_0^t \mathbf{u}_s(t') \cdot \mathbf{e}_r dt',$$

where \mathbf{e}_r is a radial unit vector. Because the vorticity is frozen to the fluid particle for a two-dimensional incompressible barotropic fluid, the above integrals represent contributions of each regions to the displacements of the vorticity contour. That is, A_c and A_s are displacements of the vorticity contour advected by the velocities induced by the core region and the surrounding region, respectively.

Fig.7 shows the evolution of A_c and A_s at the maximum curvature point of the vorticity contour, $\omega = 6, 7, 8$. A_s for all the contours rapidly decreases in $0 < t \lesssim 1.5$ and exhibits a relatively small decrease in $7 \lesssim t \lesssim 8$. As shown in section 3.1, these time intervals correspond to the intervals during filament formation. At the maximum curvature point, A_s and A_c are always negative, but the magnitude of A_c is small compared with that of A_s . On the other hand, A_s at the minimum curvature point increases during approximately the same interval when A_s at the maximum curvature point decreases (Fig.8). This indicates that the surrounding region contributes to the axisymmetrization of the elliptic vortex. The surrounding region consists of the filaments and the weak vorticity region around the vortex core. The weak vorticity region, which homogeneously surrounds the vortex core, does not contribute to the axisymmetrization because the mirror-symmetric vorticity field cannot

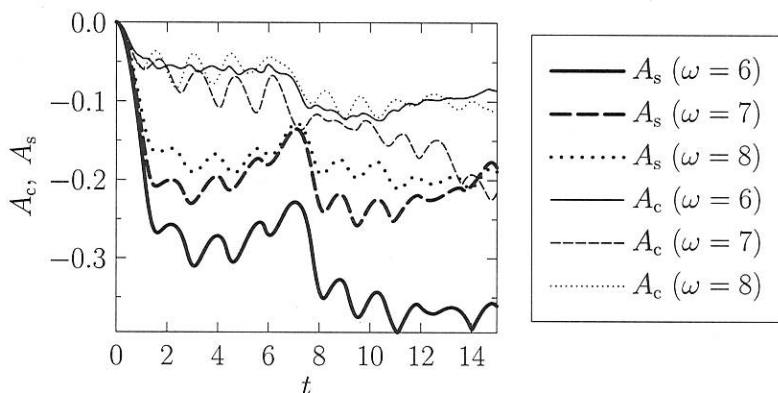


Figure 7: Time evolution of $A_c(t)$ and $A_s(t)$ at the maximum curvature point.

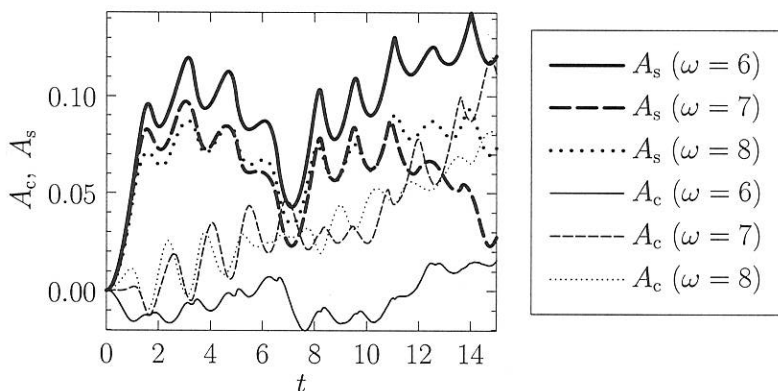


Figure 8: Time evolution of $A_c(t)$ and $A_s(t)$ at the minimum curvature point.

contribute to ϕ_d , that is, to the axisymmetrization²⁾ (Fig.9). The facts that the axisymmetrization occurs during filament formation and that the weak vorticity region is almost mirror symmetric strongly suggest that the filaments are the main cause of the axisymmetrization.

4. CONCLUSION

We have quantitatively discussed the axisymmetrization of an isolated elliptic vortex with a non-uniform vorticity distribution for a two-dimensional incompressible barotropic fluid. To investigate the role of filaments in the axisymmetrization of an elliptic vortex, we defined a core and surrounding regions. We investigated the deformations of the vorticity contours in the vortex core by velocities induced by the core and the surrounding regions. The deformations of the vorticity contours due to the surrounding region were significant, particularly when the filaments were forming. This investigation showed that the filaments substantially contributed to the axisymmetrization of the elliptic vortex.

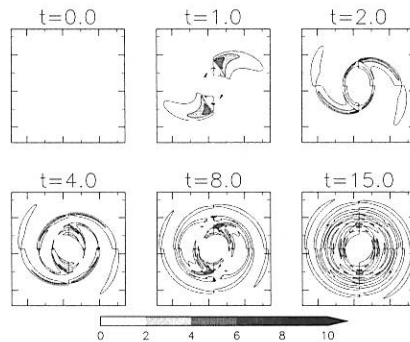


Figure 9: Snapshots of anti-mirror symmetric vorticity fields on the principal axes of the ellipse with $\omega = 6$. The coordinates are rotated so that the major axis of the ellipse with $\omega = 6$ is coincident with y -axis.

These analyses of the contribution of the surrounding region did not reveal which part of the filaments contributed the most to the axisymmetrization and how they contributed to the axisymmetrization. A study clarifying these points is currently underway and will be reported in a paper that is in preparation.

We discussed the role of filaments in the axisymmetrization for the compact-support initial vorticity distribution. We confirm that the result for the compact-support distribution, which is monotonically decreasing function with radial directions measured from the center of the vortex core, also holds for other initial vorticity distributions, such as a Gaussian distribution used by Kimura and Herring (2001)³⁾ and a discontinuous distribution used by Dritschel (1998).¹⁰⁾ A detailed analysis of initial distributions will be presented in a paper that is in preparation.

ACKNOWLEDGMENT

One of the authors (SM) has been supported by the CPS under the auspices of the MEXT GCOE Program, entitled “Foundation of the international education and research center for planetary science”. The GFD-DENNOU Library was used for drawing some figures. This work was also partly supported by a Grant-in-Aid for Scientific Research No.20540424 and 21654065 from the Japanese Society for the Promotion of Science.

REFERENCES

- 1) McWilliams, J. C., “The emergence of isolated coherent vortices in turbulent flow”, *J. Fluid Mech.*, **146** (1984), pp. 21 – 43.
- 2) Melander, M. V., McWilliams, J. C. and Zabusky, N. J., “Axisymmetrization and vorticity-gradient intensification of an isolated two-dimensional vortex through filamentation”, *J. Fluid Mech.*, **178** (1987), pp. 137 – 159.
- 3) Kimura, Y. and Herring, J. R., “Gradient enhancement and filament ejection for a non-uniform elliptic vortex in two-dimensional turbulence”, *J. Fluid Mech.*, **439** (2001), pp. 43 – 56.
- 4) Fitzgibbon, A., Pilu, M. and Fisher, R. B., “Direct Least Square Fitting of Ellipses”, *IEEE Transactions on Pattern Analysis and Machine Intelligence*, **21** (1999), pp. 476 – 480.

- 5) Okubo, A., "Horizontal dispersion of floatable particles in the vicinity of velocity singularities such as convergences", *Deep-Sea Res.*, **17** (1970), pp. 445 – 454.
- 6) Weiss, J., "The dynamics of enstrophy transfer in two-dimensional hydrodynamics", *Physica D*, **48** (1991), pp. 273 – 294.
- 7) Hua, B. L. and Klein, P., "An exact criterion for the stirring properties of nearly two-dimensional turbulence", *Physica D*, **113** (1998), pp. 98 – 110.
- 8) LaCasce, J. H., "The vortex merger rate in freely decaying, two-dimensional turbulence", *Phys. Fluids*, **20** (2008), 085102.
- 9) Iwayama, T. and Okamoto, H., "Reconsideration of a Scaling Theory in Two-Dimensional Decaying Turbulence", *Prog. Theor. Phys.*, **96** (1996), pp. 1061 – 1071.
- 10) Dritschel, D. G., "On the persistence of non-axisymmetric vortices in inviscid two-dimensional flows", *J. Fluid Mech.*, **371** (1998), pp. 141 – 155.